# Reactive Scattering of Oxygen and Nitrogen Atoms

PIERGIORGIO CASAVECCHIA,*
NADIA BALUCANI, MICHELE ALAGIA,
LAURA CARTECHINI, AND
GIAN GUALBERTO VOLPI

*Dipartimento di Chimica, Università di Perugia, 06123 Perugia, Italy*

Received June 10, 1998

## I. Introduction

Molecular oxygen and nitrogen are the two main constituents of the atmosphere and play a key role in Earth's life. The oxygen reactivity and the nitrogen inertia are well-known to chemists. When in atomic form, oxygen becomes particularly reactive, especially if excited to its first electronic state $^1$D (189.8 kJ/mol above the ground state $^3$P). Ground-state nitrogen atoms are known to be much less reactive than O atoms (for symmetry and thermodynamic reasons), but electronic excitation to the first excited state, $^2$D (227.7 kJ/mol above the ground state $^4$S), renders them also very reactive.[1−3] Excited O and N atoms exhibit a marked difference in the chemical behavior with respect to their ground states; in fact, among the various forms of energy which can be supplied to a system, the electronic excitation is quite peculiar, since it leads to potential energy surfaces (PESs) whose energy, symmetry, and topology are different from those of the ground state.[1−3] The reactions of O and N atoms (both ground and excited) are of central importance in many areas of practical interest, from atmospheric to combustion chemistry and from plasma to interstellar chemistry. Because of this, they have been extensively investigated from a kinetic standpoint.[1−5] Nevertheless, a deeper understanding of chemical phenomena requires investigation at the microscopic molecular level, which is the pursuit of reaction dynamics. The behavior of atoms and molecules during an elementary chemical reaction is revealed by observing the consequences of a single reactive collision, and this can be best done by performing a reactive scattering experiment using crossed molecular beams of the reactants.[6−8] Since its development in the 1950s, the crossed molecular beam (CMB) scattering technique, with its capability of measuring the velocity and angular distributions of the products, after having defined the velocity, approach angle, and other initial conditions of the reactants, has provided information which has played, and continues to play, a crucial role in the advancement of our understanding of the dynamics of elementary chemical reactions.[6−8]

The first CMB experiment aimed at elucidating the reaction dynamics of O atoms (with halogen molecules) dates back to 1973.[9] Since then, the dynamics of many O($^3$P)[10−12] and a few O($^1$D)[13] reactions were studied by the CMB method and also by spectroscopic techniques[14] such as infrared chemiluminescence (IC), laser-induced fluorescence (LIF) and resonance-enhanced multiphoton ionization (REMPI). These techniques have accompanied and complemented the CMB method over the last 20−30 years in the investigation of chemical reactions at the microscopic level. A peculiarity of O($^3$P) reactions is that the reactants approach on a triplet PES which intersects a singlet PES usually supporting a stable intermediate. Intersystem crossing (ISC) is then possible from the triplet to the singlet PES, making the dynamics which involve motion on the underlying singlet PES different from those involving motion only over the triplet PES.[10] Recent measurements of the reactive scattering of O($^3$P) with various alkyl iodides have indicated the occurrence of ISC.[16] Obviously, it is desirable to study the reaction of a given molecule with both O($^3$P) and O($^1$D) under the same experimental conditions and compare the triplet and singlet dynamics in order to directly explore the effect of electronic excitation and the occurrence of ISC. We have recently achieved the above by studying the reactive scattering of O($^3$P) and O($^1$D) with $H_2S$[15] and $CH_3I$[17] using a high-resolution CMB apparatus. It should be noted that the dynamics of O($^1$D) reactions with atmospherically relevant molecules are of great interest, since metastable O($^1$D) (radiative lifetime ∼150 s) is the main photolysis product of ozone in the stratosphere.[1,18]

Little is known about the reaction dynamics of nitrogen atoms.[12,19] CMB studies of N atoms have been hampered by technical difficulties[20] connected with the production of beams of sufficient intensity to carry out product angular and velocity distribution measurements. We recently succeeded in investigating the reactive scattering

Piergiorgio Casavecchia was born on January 7, 1950, in Marsciano (Perugia), Italy. He received his degree in Chemistry from the University of Perugia in 1974 and did postdoctoral work with Nobel Laureate Yuan T. Lee at the University of California at Berkeley from 1977 to 1980. He is currently Associate Professor of Physical Chemistry at the University of Perugia. His research interests include the determination of intermolecular forces and the study of the dynamics of elementary reactions by the crossed molecular beam technique.

Nadia Balucani was born on October 10, 1965, in Perugia, Italy. She received her Ph.D. from the University of Perugia, did postdoctoral work in Berkeley with R. J. Saykally, and is currently Research Associate in Chemistry at the University of Perugia.

Michele Alagia obtained his Ph.D. in Chemistry in 1995 from the University of Perugia, where he is currently doing postdoctoral work.

Laura Cartechini is a third year graduate student in Chemistry at the University of Perugia.

Gian Gualberto Volpi was born on June 1, 1928 in Roma and obtained his degree in Chemistry from the University of Rome in 1951. After spending two years at Harvard University (1955−1957), he covered a position of research fellow at the Nuclear and Radiation Chemistry Lab of the CNEN (National Committee for Nuclear Research) until 1968, when he was appointed to a chair of Chemistry at the University of Perugia. He is a member of the "Accademia Nazionale dei Lincei" and of the "Accademia Nazionale delle Scienze", also referred to as the "Accademia dei XL".

10.1021/ar9702785 CCC: $18.00 
Published on Web 02/11/1999

of N($^2$D) atoms with both inorganic[21] and organic[22] molecules by exploiting the novel capability to generate intense continuous supersonic beams of N atoms.[23] These reactions are significant in a wide variety of environments: planetary and extraplanetary atmospheres,[18] interstellar and circumstellar clouds, hydrocarbon combustion, and laboratory studies of the reactions of hydrocarbons with "active nitrogen".[5] In these environments some reactive processes leading to N-containing compounds are thought to involve N($^2$D). In particular, N($^2$D) is the second most abundant metastable species in the atmosphere (average radiative lifetime ~26 h) and is the major source of NO in the thermosphere.

A strong synergism between experiment and theory has always been pivotal to the progress recorded in the field of reaction dynamics, and also some reactions of O and N atoms, because of their importance and relative simplicity, have been approached theoretically. Specifically, the reactions O($^1$D) + $H_2$ and N($^2$D) + $H_2$ have been considered as prototypes of the so-called *insertion* reactions (which are characterized by a deep potential well between reactants and products). These two systems are becoming amenable to the same level of detailed theoretical treatment that has recently occurred for the benchmark reactions H + $H_2$,[24] F + $H_2$,[7,25] and Cl + $H_2$,[26] which follow the better understood *abstraction* mechanism.

The main thrust of our CMB work has been that of (a) further investigating the reactive scattering of oxygen atoms with a special focus on electronically excited O($^1$D)[27] and on the comparative study of O($^3$P) and O($^1$D) reaction dynamics,[15,17] (b) extending reactive scattering studies to nitrogen atoms,[21,22] (c) studying the dynamics of simple *insertion* reactions such as O($^1$D) + $H_2$ and N($^2$D) + $H_2$ in order to provide experimental data for comparison with theory,[21,28] (d) providing scattering data for Cl + $H_2$,[26] which is the only other reaction for which exact quantum scattering calculations are feasible to date, beyond H + $H_2$ and F + $H_2$, (e) extending reactive scattering studies to the chemically very important hydroxyl radical,[15,29] and (f) exploring the reactive scattering of O($^3$P,$^1$D) from a liquid surface.[30] In this Account, we review our recent accomplishments on the first three topics.

## II. The Crossed Molecular Beams Technique

The experiments were carried out in a CMB apparatus (Figure 1) which follows the classic design of Nobel laureates Lee and Herschbach[6,7] and has been described elsewhere.[15] Briefly, supersonic beams of the reagents with well-defined velocities, angular divergences, and internal quantum states are crossed at 90° in a large vacuum chamber maintained in the $10^{-7}$ mbar range. Each beam is so dilute that collisions within it are negligible; collisions occur only between a molecule of one beam and a molecule of the intersecting beam. The angular direction and velocity of the product molecules scattered from the collision zone are measured after a single and well-defined collision event using an electron-impact ionization quadrupole mass spectrometer—a universal detector—contained in a ultrahigh-vacuum chamber which can rotate in the collision plane around an axis that passes through the collision center. The pseudorandom time-of-flight (TOF) method is used for velocity distribution measurements.

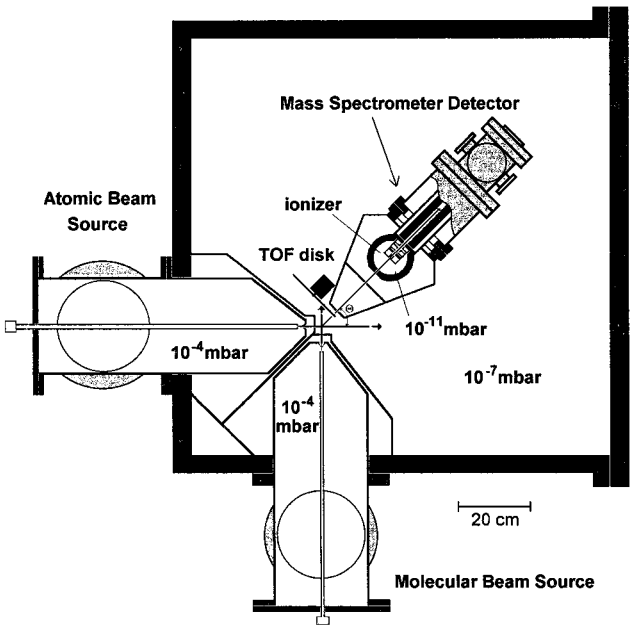


**FIGURE 1.** Crossed molecular beam instrument.

Central to the success of the studies reviewed here has been the generation of intense beams of the atomic reactants. This is done using a radio frequency discharge beam source.[15,31] With dilute (2.5−5%) mixtures of $N_2$ or $O_2$ in He or Ne gas as the starting material, high degrees of molecular dissociation are attained: the N atoms are mainly in the ground $^4$S and in the first excited $^2$D state, while most of the O atoms are found in the ground $^3$P state with a small percentage in the first excited $^1$D state.[23]

Information on the reaction dynamics is contained in the double-differential cross section in the center-of-mass (CM) system, $I(\theta,E)$ (where $\theta$ and $E$ are the scattering angle and product translational energy, respectively), which strongly depends on the nature of the PES and may be compared directly to predictions of classical and quantum-mechanical models based on collision theory.[32] $I(\theta,E)$ is derived from the analysis of the laboratory data (angular, $N(\Theta)$, and TOF, $N(\Theta,t)$, distributions) by forward convolution over the experimental conditions of trial CM angular and translational energy distributions.[7] $I(\theta,E)$ is often reported as a velocity flux contour map of the reaction products, i.e., the plot of intensity as a function of $\theta$ and CM velocity $u$. The contour map can be regarded as the reaction *image*. We recall that while the measurement of the energy distribution of reaction products is not a unique capability of the method, information on the product angular distribution of bimolecular reactions is best obtained from CMB experiments.

Reactive scattering experiments in CMB allow one[6−8] to identify the primary reaction products and explore the nature of reaction intermediates and their subsequent

decay dynamics (*direct* reactions and *long-lived complex* forming reactions). They also permit obtaining the energy partitioning of the products between translational and internal degrees of freedom, understanding the correlation between initial and final angular momenta in the reactive collision, and correlating the reaction dynamics to features of the PES. All these points are exemplified below.

The concept of *direct* reactions and *long-lived complex* forming reactions are some of the important paradigms which were established by CMB experiments (together with quasiclassical trajectory (QCT) calculations).[32] If the collision complex which is formed in any bimolecular A + BC → AB + C reactive encounter lasts a very short time only—tens of femtoseconds, the typical period of molecular vibrations—it does not have time to rotate before it breaks apart; therefore, the angular distribution of the AB product will be strongly anisotropic in the CM system and the reaction is said to be *direct*. When the AB angular distribution peaks at $\theta = 0°$ with respect to the direction of A (*forward* direction), the mechanism is *stripping*, while when it peaks at $\theta = 180°$ (*backward* direction), the mechanism is *rebound*. If the collision complex lives a time long enough—on the order of picoseconds, the typical period of molecular rotations—the complex can rotate several times before it breaks apart and, by the time it decomposes, it will have "forgotten" the directions of the incoming collision partners. The angular distribution of the products in the CM system will have backward–forward symmetry. Direct reactions are usually associated with a repulsive or weakly attractive PES, while long-lived complex forming reactions with a PES having a deep potential well between reactants and products can "trap" the complex. When the lifetime of the complex is comparable to, or slightly shorter than, its rotational period, the angular distribution becomes partially asymmetric (usually forward peaked) and the complex is called an *osculating* complex.[32] Using the rotational period as a "clock", it is possible to estimate the lifetime of the complex from the degree of asymmetry of the angular distribution, as shown below.

## III. Reactive Scattering of $O(^3P,^1D)$ with $H_2S$ and $CH_3I$: Triplet versus Singlet Dynamics

These reactions are of fundamental and practical relevance. $O + H_2S$ is a prototypical system for the oxidation/combustion processes of sulfur compounds. $O + CH_3I$ is representative of halogenated compound combustion chemistry and is of potential interest in the atmospheric chemistry of $CH_3I$ (the main source of atmospheric iodine), which has recently been proposed as a contributor to ozone destruction in the lower stratosphere. For both systems ab initio calculations on intermediates, transition states, and products have recently become available.[33]

The $O(^3P)$ reaction with $H_2S$ is known to have an activation energy of 18 kJ/mol and to be about 4 orders of magnitude slower ($k_{298} = 1.8 \times 10^{-14}$ cm$^3$ molecule$^{-1}$ s$^{-1}$) than that of $O(^1D)$. Three different reaction channels are thermodynamically open for $O(^3P,^1D) + H_2S$ leading to (1a) HSO(HOS) + H, (1b) SO + $H_2$, and (1c) OH + SH. We have examined channels 1a and 1b, while channel 1c has been investigated in other laboratories by using IC and LIF techniques. The H-displacement pathway 1a is known to be a major one (≥50%) in the reactions of both $O(^3P)$ and $O(^1D)$, while channel 1b is thought to be negligible.[34]

The reaction $O(^3P,^1D) + CH_3I$ has many thermodynamically allowed products. We have investigated the IO + $CH_3$ formation channel. This has been recently established by Ravishankara and co-workers[35] to be the dominant one ($k_{298} = 1.8 \times 10^{-11}$ cm$^3$ molecule$^{-1}$ s$^{-1}$) for the triplet reaction. The rate constant for $O(^1D) + CH_3I$ is not known but is expected to be similar to that of $O(^1D)$ + $CH_3Br$ and $CH_3Cl$ ($k_{298} \approx 2 \times 10^{-10}$ cm$^3$ molecule$^{-1}$ s$^{-1}$).

Figures 2a and 3a portray the reaction coordinate diagrams showing reactants, intermediates, and products for the HSO(HOS) + H and IO + $CH_3$ formation channels, respectively (the energetics are based on ab initio calculations by Marshall *et al.*[33]). In both cases the $O(^1D)$ reactions proceed on a singlet PES, forming an addition complex ($H_2SO$ and $CH_3IO$) or an insertion complex (HOSH and $CH_3OI$), which dissociate to products (HSO + H and IO + $CH_3$; the product HOS is also possible in the case of the HOSH complex) because of their high energy content. Isomerization between the two singlet complexes is possible. The $O(^3P)$ reactions can either proceed on the triplet PES or undergo ISC to the singlet PES, thus exploring the potential well of the singlet intermediate.

We have measured laboratory angular and TOF distributions at the mass-to-charge ratio $m/e$ 49 (HSO and/or HOS) at different collision energies ($E_c$).[15] Figure 2b shows the HSO product angular distributions at $E_c = 14.2$ (below the $O(^3P)$ threshold) and 49.4 kJ/mol (above); for the higher $E_c$ also a TOF spectrum is reported (Figure 2c). While at $E_c = 14.2$ kJ/mol the lab angular distribution is symmetric with respect to the center-of-mass position, as $E_c$ is raised above 25 kJ/mol the lab angular and TOF distributions show structures which are easily visible in parts b and c of Figure 2. These structures are unambiguously related to features of the angular and velocity distributions of the HSO product arising from the $O(^3P)$ reaction. Measurements at $m/e$ 48 indicated that channel 1b is closed also to $O(^1D)$ for $E_c$ up to 49.4 kJ/mol.

Laboratory angular and TOF distributions of the IO product were measured at two different collision energies, $E_c$ = 55.4 and 64.0 kJ/mol.[17] The lower $E_c$ angular distribution is shown in Figure 3b, together with the most probable Newton diagram, which highlights the different kinematics of the $O(^3P)$ and $O(^1D)$ reactions. On the basis of linear momentum and energy conservation, the laboratory angular range within which the IO product formed from the $O(^3P)$ reaction can be scattered is much smaller (from $\Theta = 33$ to 84°) than that of IO formed from the $O(^1D)$ reaction (see Newton diagrams in Figure 3b). Similar (smaller) Newton diagrams are also reported in Figure 2b.

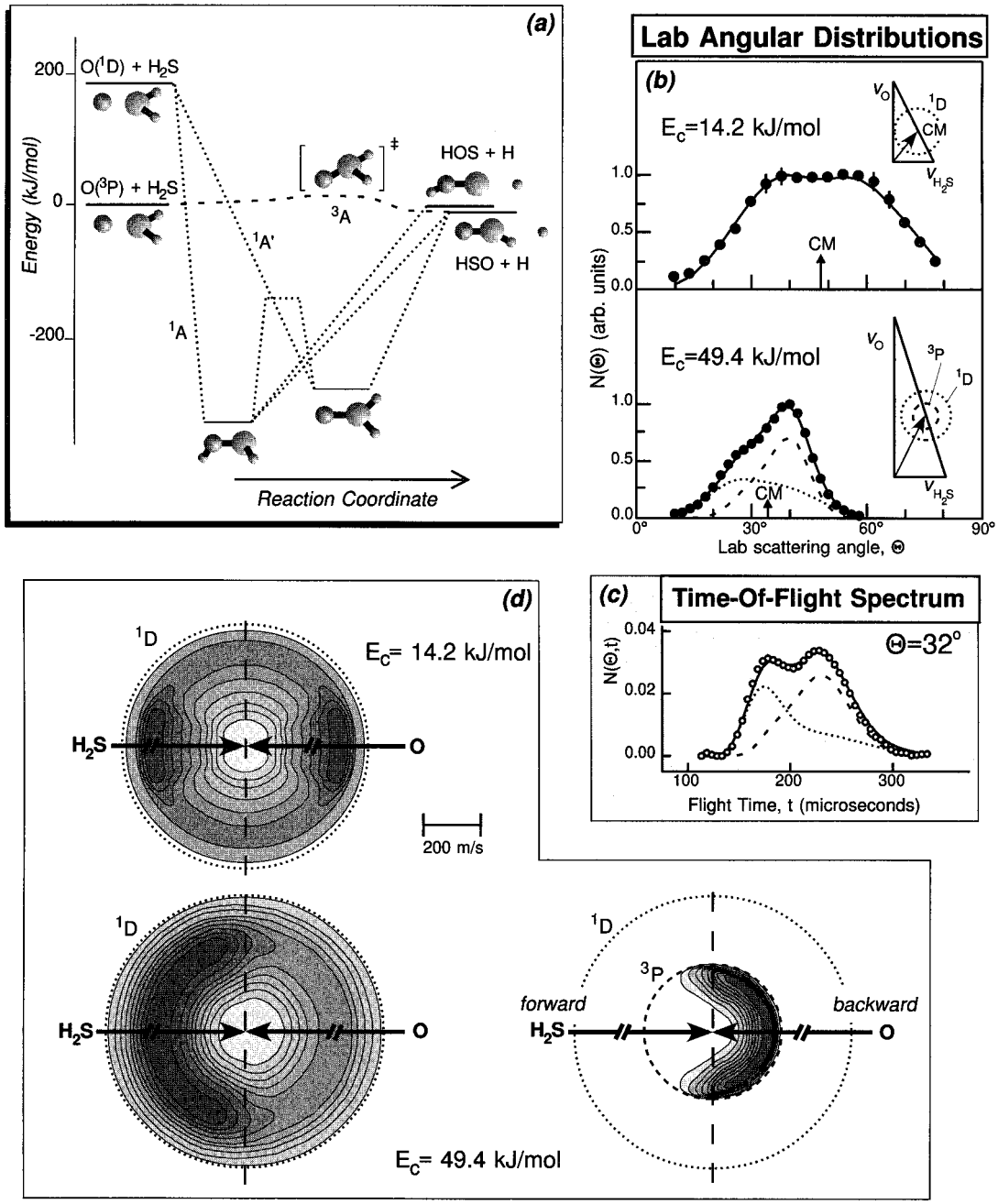


**FIGURE 2.** (a) Energy level and correlation diagram (schematic) for the $O(^3P,^1D) + H_2S$ system, relative to the H-displacement channel. (b) Laboratory angular distributions of the *m*/*e* 49 product (HSO/HOS) from $O(^1D) + H_2S$ at $E_c = 14.2$ kJ/mol and from $O(^3P,^1D) + H_2S$ at $E_c = 49.4$ kJ/mol, with Newton diagrams of the experiment also shown. Continuous curves are calculated from best-fit CM translational energy and angular distributions for $O(^1D)$ and $O(^3P)$ reactions. The separate $^1D$ and $^3P$ contributions are shown with dotted and dashed lines, respectively, at $E_c = 49.4$ kJ/mol. (c) TOF distribution of the *m*/*e* 49 product at $\Theta = 32°$ from the $O(^3P,^1D) + H_2S$ reaction at $E_c = 49.4$ kJ/mol. Symbols are as in (b). (d) Comparison between the CM flux (velocity-angle) contour maps of the HSO(HOS) product from the $O(^1D)$ reaction (left) and the $O(^3P)$ reaction (right). Note at the same $E_c$ the dramatic difference between the backward scattered flux distribution for the direct $O(^3P)$ reaction and the forward−backward distribution (with forward bias) for the osculating complex forming $O(^1D)$ reaction.

In the case of the reaction with $H_2S$, the triplet and singlet dynamics were found[15] to be dramatically different, as can be appreciated in Figure 2d, where the product contour maps are shown. At low $E_c$ the HSO (HOS) product contour map shows a symmetric backward−forward structure which is attributed to the $O(^1D)$ reaction proceeding through the formation of a long-lived complex. At higher $E_c$ the product distribution from $O(^1D)$ becomes more forward peaked (with respect to the direction of the incoming O atom), reaching a ratio $T$(backward)/$T$(forward) = 0.60 at $E_c = 49.4$ kJ/mol (see the left-hand side of Figure 2d). This indicates that the complex lifetime has decreased and the complex osculates[32] (we estimated a mean complex lifetime of 0.3 ps). A large percentage (about 40%) of the total available energy is disposed as product recoil energy in the $O(^1D)$ reaction. In contrast, the product from the $O(^3P)$ reaction at $E_c = 49.4$ kJ/mol is completely confined to the backward hemisphere and

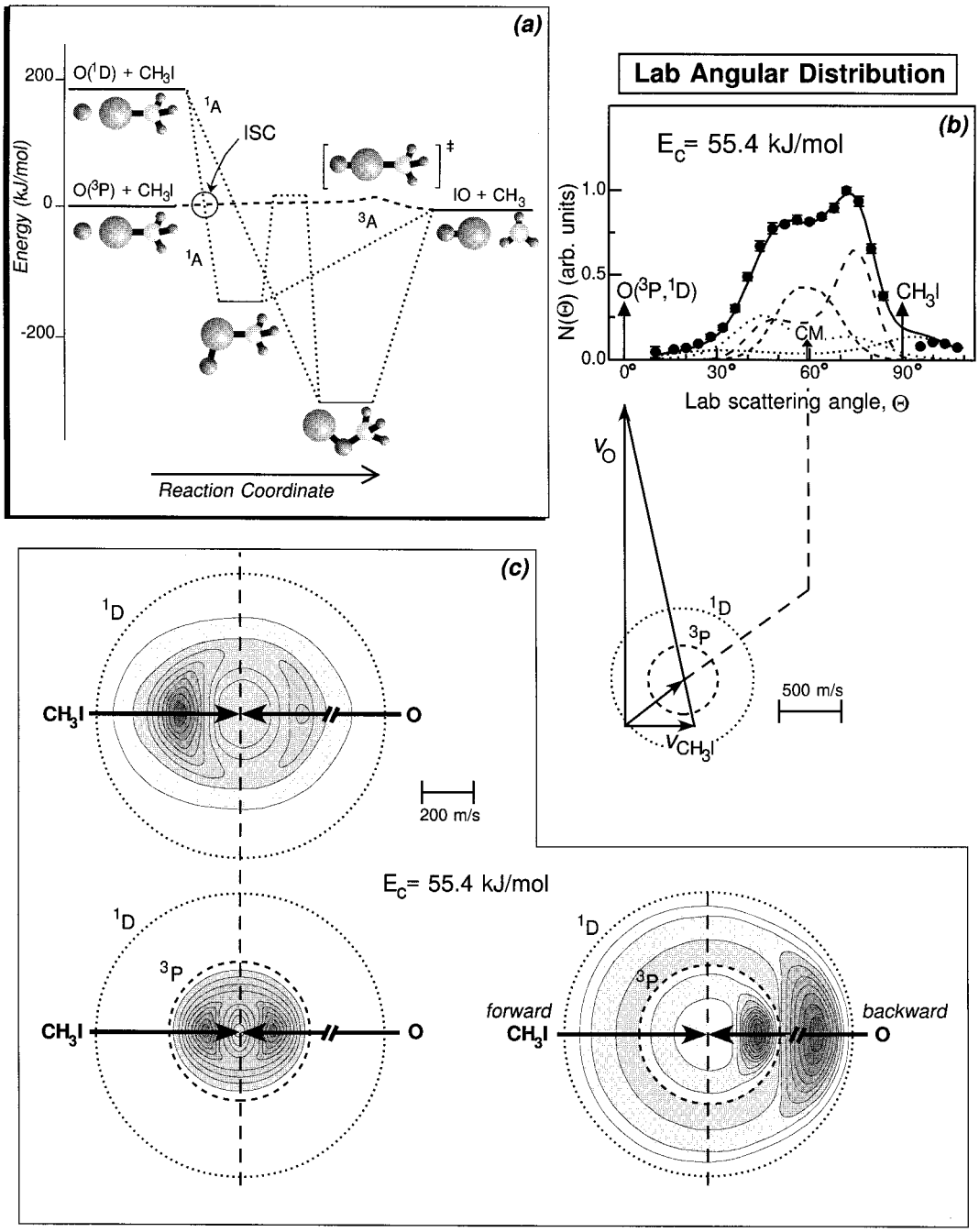


**FIGURE 3.** (a) Energy level and correlation diagram (schematic) for the $O(^3P,^1D) + CH_3I$ reactions leading to $IO + CH_3$ products. (b) Laboratory angular distribution of the IO product and corresponding Newton diagram at $E_c = 55.4$ kJ/mol. Circles denote the energetically accessible range for the $O(^3P)$ and $O(^1D)$ reactions. Curves are calculated from best-fit CM functions: (- - -) $O(^3P)$ reaction via ISC and long-lived complex; (- - -) $O(^3P)$ reaction direct; (• • •) $O(^1D)$ reaction via osculating complex; (•••) $O(^1D)$ reaction direct; (—) total. (c) CM product flux (velocity-angle) contour maps showing the IO distribution from the $O(^1D)$ reaction occurring via an osculating complex (top left), the $O(^3P)$ reaction via ISC to the singlet PES and long-lived complex formation (bottom left), and the $O(^3P)$ and $O(^1D)$ reactions occurring with direct *(*rebound*)* mechanism (bottom right).

peaks nearly at the limit of energy conservation (60% of the total available energy is found as recoil energy) (Figure 2d; right-hand side). This indicates that the reaction is direct, of the *rebound* type, and that the barrier on the triplet PES is located in the exit channel. From the translational energy release we estimated the heat of formation of the HSO radical.[36]

In the case of $O + CH_3I$ the measured distributions have features which require contributions from the $O(^3P)$ and $O(^1D)$ reactions. A detailed data analysis shows that both reactions occur through two different competitive micromechanisms.[17] As shown by the CM flux contour maps in Figure 3c, the first micromechanism for $O(^3P)$ is characterized by a symmetric backward−forward peaked angular distribution which is quite polarized (i.e., the intensity in the forward and backward directions is quite larger than that in the sideways direction) and by a product translational energy peaking at low energy. These

findings are attributed to reaction proceeding through the formation of a long-lived singlet $CH_3IO$ complex following ISC from the triplet to the singlet PES (see Figure 3a). The corresponding micromechanism of the $O(^1D)$ reaction has a forward peaked CM angular distribution with a moderate fraction of recoil energy and reflects the formation of an *osculating complex* following $O(^1D)$ addition and/or insertion on the singlet PES. The osculating complex is consistent with the much shorter complex lifetime, due to the higher exoergicity, for the $O(^1D)$ reaction with respect to the $O(^3P)$ reaction via ISC. The second micromechanism for both $O(^3P)$ and $O(^1D)$ is characterized by a preferentially backward-peaked CM angular distribution with high product recoil energy. For $O(^3P)$ this is attributed to a direct (rebound) reaction over the triplet PES and indicates that the preferred geometry for reaction is nearly collinear O−I−$CH_3$. For $O(^1D)$ it may be attributed either to ISC from the singlet to the triplet PES or to small impact parameter collisions on the singlet PES. The four separate contributions to the total angular distribution are shown in Figure 3b. The resulting weight of the $O(^1D)$ contribution to the total CM product flux is comparable to that of $O(^3P)$ and reflects the higher reactivity but lower concentration in the beam of $O(^1D)$ with respect to $O(^3P)$. The ratio of cross sections between the triplet reaction via ISC and the direct triplet reaction is ∼1. These findings are corroborated by very recent ab initio calculations on the $O(^3P,^1D) + CH_3I$ system which highlight the role of ISC for bent geometry[33] and are in line with the results obtained by Grice and co-workers[16] in studies of a series of $O(^3P)$ + alkyl iodide reactions.

A comparison between the two systems points to one striking difference: ISC is seen to occur in the case of the $CH_3I$ reaction, while it is absent in the case of $H_2S$. This can be rationalized by the presence of the heavy iodine atom, which strongly facilitates the occurrence of ISC. Another difference is given by the different degree of the angular distribution polarizations for the two $O(^1D)$ reactions. We can explain that on the basis of angular momentum partitioning arguments.[32] In the case of HOSH/$H_2SO$ decomposing to HSO(HOS) + H, since the departing H atom is a light particle, it will not carry away a significant fraction of the total angular momentum and the rotational energy of the complex will mainly appear as rotational excitation of the product, giving a mild polarization of the CM angular distribution. In the decomposition of $CH_3IO$, however, a significant fraction of the angular momentum will be carried away by the departing $CH_3$ radical, since the departing $CH_3$ has the same mass of the O atom which attaches to $CH_3I$, generating a strongly polarized angular distribution and weak product rotational excitation.

## IV. Reactions of $O(^1D)$ and $N(^2D)$ with $H_2$

The simplest reactions of $O(^1D)$ and $N(^2D)$, those with molecular hydrogen

$$O(^1D) + H_2(^1\Sigma^+) \rightarrow OH(X^2\Pi) + H(^2S) \qquad \Delta H^\circ_0 = -179.6 \text{ kJ/mol} \quad (1)$$

$$N(^2D) + H_2(^1\Sigma^+) \rightarrow NH(X^3\Sigma^-) + H(^2S) \qquad \Delta H^\circ_0 = -139.0 \text{ kJ/mol} \quad (2)$$

are of great practical and fundamental interest. Figure 4a portrays schematic energy level and correlation diagrams based on new high-quality PESs very recently developed for these two reactions using accurate ab initio electronic structure calculations.[21,37] It should be noted that the corresponding reaction with $H_2$ of the ground-state atoms either has a large energy barrier (∼37 kJ/mol for $O(^3P)$) or is strongly endoergic ($\Delta H^\circ_0$ = 88.7 kJ/mol for $N(^4S)$); hence, they do not occur at low collision energies. As can be seen from Figure 4a, the two reactions share considerable similarities: the lowest PES correlates adiabatically with a very stable intermediate (the ground states of the water molecule and of the amidogen radical, respectively), the exoergicities are similar, and a manifold of PESs (not all depicted) correlate with the reactants. The notable difference is that, for collinear geometry, the ground-state $^1\Sigma$ PES of $O(^1D) + H_2$ does not correlate with ground-state products—but the first excited $^1\Pi$ PES ($^1A''$ and $2^1A'$ in $C_s$ geometry) does. In contrast, for $N(^2D) + H_2$ the ground-state $^2\Sigma$ PES ($^2A''$ in $C_s$ geometry) does correlate with ground-state products, while the excited states $^2\Delta$ and $^2\Pi$ are very repulsive.

We have undertaken a simultaneous study of $O(^1D) + H_2$ and $N(^2D) + H_2$ and have compared the experimental results with those of dynamic calculations by the QCT method on the new ab initio PESs.[21,28,38] We have studied the reactions of $O(^1D)$ with $H_2$ and $D_2$[28] and that of $N(^2D)$ with only $D_2$ for technical reasons.[21] Figure 4b shows the lab angular distributions of the OD product from reaction 1 at $E_c$ = 22.2 kJ/mol and of the ND product from reaction 2 at $E_c$ = 21.3 kJ/mol. Note that in the two experiments the $D_2$ beam is the same and the $O(^1D)$ and $N(^2D)$ velocities are very similar; hence, the kinematics are nearly identical. However, as can be directly seen from the laboratory data, there exists a pronounced difference between the two angular distributions. They are both centered around the CM angle but appear to have an opposite behavior, with OD exhibiting more intensity on the right of the CM angle and ND having more intensity on the left of the CM angle. The angular distributions in the CM are reported in Figure 4c (solid lines); product translational energy distributions, not shown here, witness a fraction of the total available energy released as product translation of about 30% in both cases. Figure 4c shows that the experimental OD angular distribution has more intensity in the backward direction ($\theta$ = 180°) (with respect to the O atom) than in the forward direction ($\theta$ = 0°), while that of ND is nearly symmetric. While QCT calculations using the $^2A''$ ground-state PES of $NH_2$ give a good agreement with experiment,[21] QCT calculations using the $^1A'$ ground-state PES of $H_2O$ underestimate the experimental results in the backward direction. Notably, QCT calculations including also the first excited PES $^1A''$

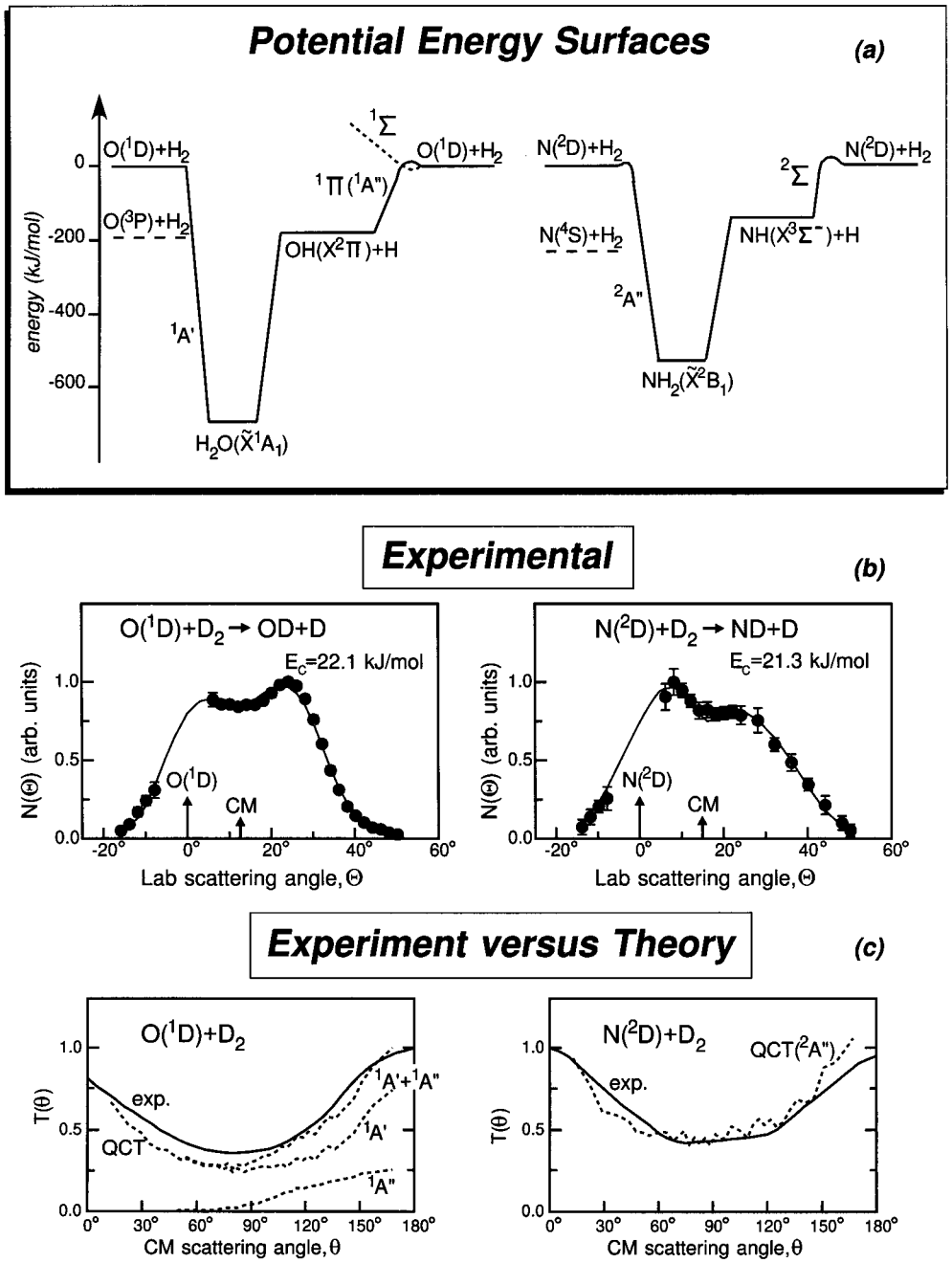


**FIGURE 4.** (a) Energy level and correlation diagrams (schematic) for the $O(^1D) + H_2$ and $N(^2D) + H_2$ reactions showing the perpendicular and collinear approaches of the atoms to $H_2$. The energy scales are the same for the two systems. (b) Laboratory angular distributions of the OD and ND products at the comparable collision energies indicated. (c) Experimental (continuous line) OD and ND angular distributions in the CM system compared to predictions from QCT calculations on the ground $^2A''$ PES for $N(^2D) + H_2$ and on the ground $^1A'$ and first excited $^1A''$ PES for $O(^1D) + H_2$.

of $H_2O$ lead to an improved agreement with the experiment, as can be seen from Figure 4c.[38] Therefore, we might interpret the CM angular distribution of the OD product in terms of a direct *abstraction* mechanism (giving a backward scattered product CM angular distribution) superimposed to a predominant *insertion* mechanism (giving a symmetric CM angular distribution), with abstraction taking place on the first excited PES $^1A''$ ($^1\Pi$ in collinear geometry) which has a barrier of 10 kJ/mol (see Figure 4a).[28,37,38] A similar interpretation was proposed by Liu and co-workers[39] from CMB studies with H/D REMPI detection of the excitation function for $O(^1D) +$ $H_2$, $D_2$, and HD. In the case of $N(^2D) + H_2$, an analogous excited PES (in collinear geometry) correlating adiabatically with ground-state products is not present (see Figure 4a), and this may explain the absence of a direct *abstraction* contribution.

## V. Conclusions

We have briefly described how reactive scattering studies by the CMB method can provide detailed information about the reaction dynamics of the chemically important oxygen and nitrogen atoms. By measuring the angular and

velocity distributions of the reaction products, we have been able to identify the primary reaction products, characterize their dynamics of formation, learn about the disposal of angular momentum in the products and therefore about details of the mechanism at the molecular level. We have also explored what is the effect of electronic excitation of the atom on the reaction dynamics and what is the extent of ISC in $O(^3P)$ reactions. From all that we have learned about the features of the PESs governing the reactions. When these reactions involve a light species such as $H_2$, modern quantum chemistry can provide from first principles accurate PESs and we can compare the experimental scattering quantities with those calculated on the PESs and test their reliability.

The examples shown also witness some of the current capabilities of the CMB method. These experiments, together with the contribution from complementary investigations using pump-probe spectroscopic techniques and beam-laser methods and from improved theoretical calculations, will hopefully further deepen our understanding of O and N atom reaction dynamics in the coming years.

*Financial contributions of the Italian "Consiglio Nazionale delle Ricerche" and "Ministero Università e Ricerca Scientifica", the European Commission through the TMR program (Contract No. FMRX-CT97-0132), and the Air Force Office of Scientific Research through the European Office of Aerospace Research and Development (Grant No. SPC-94-4042) are gratefully acknowledged.*

## References

(1) Schofield, K. Critically evaluated rate constants for gaseous reactions of several electronically excited species. *J. Phys. Chem. Ref. Data* **1979**, *8*, 723−798.
(2) Donovan, R. J.; Husain, D. Recent advances in the chemistry of electronically excited atoms. *Chem. Rev.* **1970**, *70*, 489−516.
(3) Suzuki, T.; Shihira, Y.; Sato, T.; Umemoto, H.; Tsunashima, S. Reactions of $N(2^2D)$ and $N(2^2P)$ with $H_2$ and $D_2$. *J. Chem. Soc., Faraday Trans.* **1993,** *89*, 995−999.
(4) Baulch, D. L.; Cobos, C. J.; Cox, R. A.; Esser, C.; Frank, P.; Just, Th.; Kerr, J. A.; Pilling, M. J.; Troe, J.; Walker, R. W.; Warnatz, J. Evaluated kinetic data for combustion modelling. *J. Phys. Chem. Ref. Data* **1992**, *21*, 411−734. Atkinson, R.; Baulch, D. L.; Cox, R. A.; Hampson, Jr., R. F.; Kerr, J. A.; Rossi, M. J. Evaluated kinetic and photochemical data for atmospheric chemistry: Supplement VI. *J. Phys. Chem. Ref. Data* **1997**, *26*, 1329−1499.
(5) Kistiakowsky, G. B.; Volpi, G. G. Reactions of nitrogen atoms. I. Oxygen and oxides of nitrogen. *J. Chem. Phys.* **1957**, *27*, 1141−1149. Reaction of nitrogen atoms. II. $H_2$, CO, $NH_3$, NO, and $NO_2$. *J. Chem. Phys.* **1958,** *28*, 665−668. Wright, A. N.; Winkler, C. A. *Active Nitrogen;* Academic Press: New York, 1968. Lin, C. L.; Kaufman, F. Reactions of metastable nitrogen atoms. *J. Chem. Phys.* **1971**, *55*, 3760−3770. Stief, L. J.; Nesbitt, F. L.; Payne, W. A.; Kuo, S. C.; Tao, W.; Klemm, R. B. Rate constant and reaction channels for the reaction of atomic nitrogen with the ethyl radical. *J. Chem. Phys.* **1995**, *102*, 5309−5316 and references therein.
(6) Herschbach, D. R. Molecular dynamics of elementary chemical reactions. In *Nobel Lectures in Chemistry 1981−1990*; Frängsmyr, T., Malstrom, B. G., Eds.; World Scientific: Singapore, 1992; pp 265−314. Lee, Y. T. Molecular beam studies of elementary chemical processes. In *Nobel Lectures in Chemistry 1981−1990*; Frängsmyr, T., Malstrom, B. G., Eds.; World Scientific: Singapore, 1992; pp 320−357.
(7) Lee, Y. T. Molecular beam studies of elementary chemical processes. *Science* **1987**, *236*, 793−798. Lee, Y. T. Reactive scattering I: Nonoptical methods. In *Atomic and Molecular Beam Methods*; Scoles, G., Ed.; Oxford University Press: New York, 1987; Vol. 1.
(8) Casavecchia, P. An intimate view of chemical reactions. *Science Spectra* **1996**, No. 6, 56−63.
(9) Parrish, D. D.; Herschbach, D. R. Molecular beam chemistry: Persistent collision complex in reaction of oxygen atoms with bromine molecules. *J. Am. Chem. Soc.* **1973**, *95*, 6133−6134.
(10) Grice, R. Reactive scattering of ground-state oxygen atoms. *Acc. Chem. Res.* **1981**, *14*, 37−42.
(11) Schmoltner, A. M.; Chu, P. M.; Lee, Y. T. Crossed molecular beam study of the reaction $O(^3P) + C_2H_2$. *J. Chem. Phys.* **1989**, *91*, 5365−5373 and references therein.
(12) Whitehead, J. C. The distribution of energy in the products of simple reactions. In *Comprehensive Chemical Kinetics*; Bamford, C. H., Tipper, C. F. H., Eds.; Elsevier: Amsterdam, 1983; Vol. 24, Chapter 5.
(13) Buss, R.; Casavecchia, P.; Hirooka, T.; Sibener, S. J.; Lee, Y. T. Reactive scattering of $O(^1D) + H_2$. *Chem. Phys. Lett.* **1981**, *82*, 386−391.
(14) An extensive list of references to studies of O atom reaction dynamics using spectroscopic techniques can be found in ref 15.
(15) Alagia, M.; Balucani, N.; Casavecchia, P.; Stranges, D.; Volpi, G. G. Reactive scattering of atoms and radicals. *J. Chem. Soc., Faraday Trans.* **1995**, *91*, 575−596 and references therein.
(16) Gao, X.; Essex-Lopresti, J.; Munro, S.; Hall, M. P.; Smith, D. J.; Grice, R. Role of Renner Teller and spin−orbit interaction in the dynamics of the $O(^3P) + CH_2ICl$ reaction. *J. Phys. Chem. A* **1998**, *102*, 1912−1917 and references therein.
(17) Alagia, M.; Balucani, N.; Cartechini, L.; Casavecchia, P.; van Beek, M.; Volpi, G. G. Crossed beam studies of the $O(^3P,^1D) + CH_3I$ reactions: Direct evidence of intersystem crossing for bent geometry. *Faraday Discuss.*, *113*, in press.
(18) Wayne, R. P. *Chemistry of Atmospheres*; Clarendon Press: Oxford, U.K., 1985.
(19) Dodd, J. A.; Lipson, S. J.; Flanagan, D. J.; Blumberg, W. A. M.; Person, J. C.; Green, B. D. $NH(X^3\Sigma^-, v=1-3)$ formation and vibrational relaxation in electron-irradiated $Ar/N_2/H_2$ mixtures. *J. Chem. Phys.* **1991**, *94*, 4301−4310. Umemoto, H.; Asai, T.; Kimura, Y. Nascent rotational and vibrational state distributions of $NH(X^3\Sigma^-)$ and $ND(X^3\Sigma^-)$ produced in the reactions of $N(^2D)$ with $H_2$ and $D_2$. *J. Chem. Phys.* **1997**, *106*, 4985−4991 and references therein.
(20) Love, R. L.; Herrmann, J. M.; Bickes, R. W.; Bernstein, R. B. Direct observation of the crossed beam (bimolecular) reaction of atomic nitrogen with halogens. *J. Am. Chem. Soc.* **1977**, *99*, 8316−8317. Porter, R. A. R.; Brown, G. R.; Grosser, A. E. Angular distribution of reaction products from the elementary reaction $N+NO_2 \rightarrow N_2O+O$ by crossed molecular beams. *Chem. Phys. Lett.* **1979**, *61*, 313−314.

(21) Alagia, M.; Balucani, N.; Cartechini, L.; Casavecchia, P.; Volpi, G. G.; Pederson, L. A.; Schatz, G. C.; Lendvay, G.; Harding, L. B.; Hollebeek, T.; Ho, T.-S.; Rabitz, H. Exploring the dynamics of nitrogen atom reactions: A combined experimental and theoretical study. To be submitted for publication.
(22) Alagia, M.; Balucani, N.; Cartechini, L.; Casavecchia, P.; Volpi, G. G.; Takayanagi, T.; Kurosaki, Y. A combined crossed beams and theoretical study of the reaction $N(^2D)+C_2H_2$. To be submitted for publication.
(23) Alagia, M.; Aquilanti, V.; Ascenzi, D.; Balucani, N.; Cappelletti, D.; Cartechini, L.; Casavecchia, P.; Pirani, F.; Sanchini, G.; Volpi, G. G. Magnetic analysis of supersonic beams of atomic oxygen, nitrogen, and chlorine generated from a radio-frequency discharge. *Isr. J. Chem.* **1997**, *37*, 329−342.
(24) Schnieder, L.; Seekamp-Rahn, K.; Wrede, E.; Welge, K. H. Experimental determination of quantum state resolved differential cross sections for the hydrogen exchange reaction $H+D_2\rightarrow HD+D$. *J. Chem. Phys.* **1997**, *107*, 6175−6195 and references therein.
(25) Manolopolous, D. E.; Stark, K.; Werner, H.-J.; Arnold, D. W.; Bradforth, S. E.; Neumark, D. M. The transition state of the $F+H_2$ reaction. *Science* **1993**, *262*, 1852−1855. Castillo, J. F.; Manolopoulos, D. E.; Stark, K.; Werner, H.-J. Quantum mechanical angular distributions for the $F+H_2$ reaction. *J. Chem. Phys.* **1996**, *104*, 6531−6546.
(26) Alagia, M.; Balucani, N.; Cartechini, L.; Casavecchia, P.; van Kleef, E. H.; Volpi, G. G.; Aoiz, F. J.; Banares, L.; Schwenke, D. W.; Allison, T. C.; Mielke, S. L.; Truhlar, D. G. Dynamics of the simplest chlorine atom reaction: An experimental and theoretical study. *Science* **1996**, *273*, 1519−1522.
(27) Alagia, M.; Balucani, N.; Casavecchia, P.; Volpi, G. G. A crossed molecular beam study of the reaction $O(^1D) + HI \rightarrow IO + H$. *J. Phys. Chem. A* **1997**, *101*, 6455−6462 and references therein.
(28) Alagia, M.; Balucani, N.; Cartechini, L.; Casavecchia, P.; van Kleef, E. H.; Volpi, G. G.; Kuntz, P. J.; Sloan, J. J. Crossed molecular beam and quasiclassical trajectory studies of the dynamics of the $O(^1D)+H_2$-$(D_2)$ reaction. *J. Chem. Phys.* **1998**, *108*, 6698−6708.
(29) Alagia, M.; Balucani, N.; Casavecchia, P.; Stranges, D.; Volpi, G. G.; Clary, D. C.; Kliesch, A.; Werner, H.-J. The dynamics of the reaction $OH+D_2\rightarrow$ HOD+D: Crossed beam experiments and quantum mechanical scattering calculations on ab initio potential energy surfaces. *Chem. Phys.* **1996**, *207*, 389−409.
(30) Garton, D. J.; Minton, T. K.; Alagia, M.; Balucani, N.; Casavecchia, P.; Volpi, G. G. Reactive scattering of ground state and electronically excited oxygen atoms on a liquid hydrocarbon surface. *Faraday Discuss.* **1997**, *108*, 387−399.
(31) Sibener, S. J.; Buss, R. J.; Ng, C. Y.; Lee, Y. T. Development of a supersonic $O(^3P_J)$, $O(^1D_2)$ atomic oxygen nozzle beam source. *Rev. Sci. Instrum.* **1980**, *51*, 167−182.
(32) Levine, R. D.; Bernstein, R. B. *Molecular Reaction Dynamics and Chemical Reactivity*; Oxford University Press: New York, 1987.
(33) Misra, A.; Berry, R. J.; Marshall, P. Potential energy surfaces for the reaction of O atoms with $CH_3I$: Implications for thermochemistry and kinetics. *J. Phys. Chem. A* **1997**, *101*, 7420−7425. Goumri, A.; Rocha, J.-D. R.; Laasko, D.; Smith, C. E.; Marshall, P. Computational studies of the potential energy surface for $O(^1D)+H_2S$: Characterization of pathways involving $H_2SO$, HOSH, and $H_2OS$. *J. Chem. Phys.* **1994**, *101*, 9405−9411. Computational studies of the potential energy surface for $O(^3P)+H_2S$: Characterization of transition states and the enthalpy of formation of HSO and HOS. *J. Chem. Phys.* **1995**, *102*, 161−169.
(34) For references to kinetics and previous dynamics work on $O + H_2S$, see ref 15.
(35) Gilles, M. K.; Turnipseed, A. A.; Talukdar, R. K.; Rudich, Y.; Villalta, P. W.; Huey, L. G.; Burkholder, J. B.; Ravishankara, A. R. Reactions of $O(^3P)$ with alkyl iodides: Rate coefficients and reaction products. *J. Phys. Chem.* **1996**, *100*, 14005−14015.
(36) Balucani, N.; Casavecchia, P.; Stranges, D.; Volpi, G. G. The enthalpy of formation of the HSO radical. *Chem. Phys. Lett.* **1993**, *211*, 469−472.
(37) Schatz, G. C.; Papaioannou, A.; Pederson, L. A.; Harding, L. B.; Ho, T.-S.; Hollebeek, T.; Rabitz, H. A global A-state potential surface for $H_2O$: Influence of excited states on the $O(^1D)+H_2$ reaction. *J. Chem. Phys.* **1997**, *107*, 2340−2350.
(38) Alagia, M.; Balucani, N.; Cartechini, L.; Casavecchia, P.; van Kleef, E. H.; Volpi, G. G.; Harding, L.; Rabitz, H.; Hollebeek, T.; Ho, T.-S.; Pederson, L. A.; Schatz, G. C., Comment in *Faraday Discuss.* **1997**, *108*, 434−435.
(39) Hsu, Y.-T.; Wang, J.-H., Liu, K. Reaction dynamics of $O(^1D)+H_2$, $D_2$, and HD: Direct evidence for the elusive abstraction pathway and the estimation of its branching. *J. Chem. Phys.* **1997**, *107*, 2351−2356.

AR9702785